Lack of p21 expression links cell cycle control and appendage regeneration in mice

Khamilia Bedelbaeva[a,1], Andrew Snyder[a,1,2], Dmitri Gourevitch[a], Lise Clark[a], Xiang-Ming Zhang[a], John Leferovich[a], James M. Cheverud[b], Paul Lieberman[a], and Ellen Heber-Katz[a,3]

[a]Cellular and Molecular Oncogenesis and Gene Expression, The Wistar Institute, Philadelphia, PA 19104; and [b]Department of Anatomy and Neurobiology, Washington University, St. Louis, MO 63110

Communicated by Hilary Koprowski, Thomas Jefferson University—Jefferson Medical College, Philadelphia, PA, February 12, 2010 (received for review November 10, 2009)

Animals capable of regenerating multiple tissue types, organs, and appendages after injury are common yet sporadic and include some sponge, hydra, planarian, and salamander (i.e., newt and axolotl) species, but notably such regenerative capacity is rare in mammals. The adult MRL mouse strain is a rare exception to the rule that mammals do not regenerate appendage tissue. Certain commonalities, such as blastema formation and basement membrane breakdown at the wound site, suggest that MRL mice may share other features with classical regenerators. As reported here, MRL fibroblast-like cells have a distinct cell-cycle (G2/M accumulation) phenotype and a heightened basal and wound site DNA damage/repair response that is also common to classical regenerators and mammalian embryonic stem cells. Additionally, a neutral and alkaline comet assay displayed a persistent level of intrinsic DNA damage in cells derived from the MRL mouse. Similar to mouse ES cells, the p53-target p21 was not expressed in MRL ear fibroblasts. Because the p53/p21 axis plays a central role in the DNA damage response and cell cycle control, we directly tested the hypothesis that p21 down-regulation could functionally induce a regenerative response in an appendage of an otherwise nonregenerating mouse strain. Using the ear hole closure phenotype, a genetically mapped and reliable quantitative indicator of regeneration in the MRL mouse, we show that the unrelated Cdkn1a$^{tmi/Tyj}$/J p21$^{-/-}$ mouse (unlike the B6129SF2/J WT control) closes ear holes similar to MRL mice, providing a firm link between cell cycle checkpoint control and tissue regeneration.

G2/M checkpoint | MRL mouse | regeneration | DNA damage | DNA repair

The ability to regenerate appendages is generally considered to be a property of organisms other than mammals, which typically heal wounds by the process of repair characterized by wound site contraction and closure with a scar. On the other hand, the replacement of limbs in the adult newt and the axolotl, for example, after injury or amputation begins with the formation of a blastema, a structure with highly proliferative cells that grows until that appendage is replaced without scarring (1, 2). The ability of blastemal cells in the adult to proliferate until normal architecture with appropriate differentiation into multiple cell types is achieved is a defining feature of regeneration.

The MRL mouse and its close relatives ("healer" strains) have unique healing and regenerative capabilities, including the complete closure and tissue regeneration of through-and-through ear hole puncture wounds with the formation of a circular blastema (3), the regrowth of articular cartilage (4), and the partial regeneration of amputated digits (5, 6).

Genetic mapping of the healing trait using microsatellite and SNP mapping indicates that the MRL healing phenotype is distributed among over 20 loci on multiple chromosomes (7–11). At the current time, the delineation of such a complex phenotype remains elusive. We thus searched for mechanisms and insights by considering previously observed but disparate findings among classical regenerating species such sponges, hydra, planaria, and newt and in cases of limited regeneration (i.e., liver) in mammals.

Sponges and hydra are classic model species used in the study of wound healing, regeneration, allograft rejection, and innate immunity (12). These organisms belong to two of the oldest metazoan lineages in the fossil record and provide molecular and cellular insight into the first evolutionary strategies used by multicellular animals to repair tissue injury and respond to microbial infection. In the case of sponges, the ability to heal injuries and regenerate lost tissue, and the ability to recognize and reject foreign tissue are both associated with the activation of a DNA damage response characterized by increased single-strand scission and the appearance of ribosubstitution and other alkali-labile sites in DNA (13).

In hydra, cells undergo programmed developmental replacement leading to an apparent indefinite lifespan (14). Hydra have a large number of regenerative cells such as interstitial gland cells (15), epithelial cells (16, 17), and cells in the foot (18), which have been shown to exhibit a unique cell-cycle phenotype characterized by G2/M bias. Adult urodele amphibians (e.g., the newt), which can regenerate many of their tissues, initiate cell cycle reentry, local dedifferentiation, and proliferation (2). Interestingly, in culture, myotubes derived from the newt showed serum stimulation driving the myotubes into S phase and arrest in G2 (19). In the regenerative mammalian liver, G2 arrest is a dominant feature in adult hepatocytes, where up to 70% are tetraploid (20). Finally stem cells also show a preference for G2/M arrest (21–23).

We thus initially focused our attention on cell cycle variation as a possible commonality and predictor of regenerative capacity. If this were the case, then we would expect that the MRL mouse would display an uncommon profile of cell cycle variation. Furthermore, we would expect the same of congenic strains in which the MRL healing phenotype is bred into a nonhealing strain, and we would expect the same of the major ancestral mouse strain of the MRL, the LG mouse, which displays the regenerating phenotype as well.

Finally, even if the above hypothesis is correct, it is not at all obvious whether cell cycle variation would be displayed only after injury is initiated and the regenerative response begun or whether these differences would exist in the basal, uninjured state as seen in the hydra.

In the present study, fibroblasts obtained from multiple regenerating (healer) and nonregenerating (nonhealer) mouse strains, recombinant inbred (RI) lines (24), and congenic mice,

Author contributions: P.L. and E.H.-K. designed research; K.B., A.S., D.G., L.C., X.-M.Z., and J.L. performed research; J.M.C. contributed new reagents/analytic tools; A.S., P.L., and E.H.-K. analyzed data; and E.H.-K. wrote the paper.

The authors declare no conflict of interest.

[1]K.B. and A.S. contributed equally to this work.

[2]Present address: TargAnox, Inc., Cambridge, MA 02138.

[3]To whom correspondence should be addressed. E-mail: heberkatz@wistar.org.

This article contains supporting information online at www.pnas.org/cgi/content/full/1000830107/DCSupplemental.

were examined for their cell cycling properties. It was noted that distinct differences were found between healers and nonhealers in the fraction of cells in G2/M. Further analysis showed a DNA damage response with increased levels of phosphorylated H2AX, an indicator of DNA double strand breaks (DSB) and p53 responses. Direct analysis of DNA damage using comet analysis showed damage in most of the healer cells.

Given the level of endogenous DNA damage and a G2 accumulation of cells in culture, we explored the possibility of a G1 cell cycle checkpoint deficiency. A member of the pathway that maintains a strong G1 checkpoint is the p53-dependent p21 cyclin dependent kinase inhibitor protein. An analysis of p21 expression showed reduced levels in healer cells. To examine the effect of p21 deficiency in tissue regeneration, ear hole closure was tested in a p21-deficient mouse. The results showed that such mice responded like MRL "healer" mice with complete ear hole closure, leading to the conclusion that a G1 checkpoint defect is associated with tissue regeneration in mice.

Results

G2/M Accumulation in Cells from Healer Mice. Because models of tissue regeneration have implicated cell cycle control mechanisms as a potential common feature among cells capable of tissue regeneration, we examined the cell cycle profile of cells cultured from normal uninjured ear tissue derived from adult healer mice. For this purpose, we used healer MRL and LG/J mice, a congenic line selected for healing (Fig. S1), healer and nonhealer recombinant inbred (RI) lines generated from LG/J healer and SM/J nonhealer mice (24), and nonhealer B6 and SM/J mice. MRL shares 75% of its genome with LG/J, having been produced by two final backcrosses to LG/J (25). We analyzed the cell cycle profile from the in vitro cultured cells of MRL healer and related strains to determine whether the profiles were different from control nonhealer mice. Using standard propidium iodide DNA content labeling and flow cytometry analysis, cell cycle profiles were compared, and the healer cells showed a definitive accumulation in the G2/M phase versus control cells (Fig. 1). Four different pairs of cells were used and all showed a similar accumulation (Table S1). The most dramatic differences were observed when the RI healer and nonhealer strains and the congenic and B6 strains were compared. In the nonhealers, the profile was consistent with what is generally observed in a normal mouse cell population in that the majority of cells were in G1 phase, with smaller percentages seen in S-phase and G2/M. In contrast, the healer cells and in particular the RI line 6 showed 21.5% of cells in G0/G1, whereas 64.1% of cells were in G2/M phase. The pronounced accumulation of cells in G2/M was consistent with that observed in other models of regeneration suggesting that cell cycle control mechanisms are associated with cellular regenerative potential.

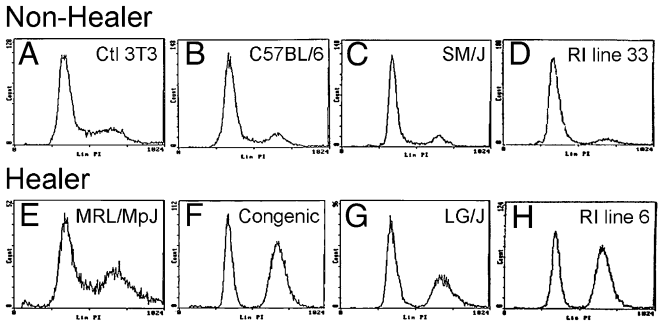

Fig. 1. Cell cycle analysis of nonhealer and healer ear-derived cells. (*A*) Control cells (NIH 3T3); (*B–D*) dermal cells derived from the ear pinnae of nonhealer B6, SM/J, and RI line 33, respectively; (*E–H*) healer MRL/MpJ, congenic, LG/J, and RI line 6, respectively, were seeded at the same number and grown for 3 days. Cells were harvested and labeled with propidium iodide and analyzed by flow cytometry analysis for stage of cell cycle, G0/G1, S, G2/M. The *y* axis shows the number of cells counted and the *x* axis shows an increasing amount of propidium iodide incorporation/cell (*Left* to *Right*).

Expression and Stabilization of p53 in MRL Healer Cells in Vitro and in Vivo. The G2/M transition is regulated by a complex series of molecular interactions that can elicit a cell cycle checkpoint that may involve the tumor suppressor p53 protein. To determine if p53 was involved, two different methods were used to assess p53 expression levels (Fig. 2). First, in vitro experiments were carried out with MRL and congenic cells derived from normal uninjured ear tissue compared to nonhealer B6 cells for steady state levels of p53 protein. MRL and healer congenic cells had readily detectable levels of p53, although little or no p53 was detected in B6 (Figs. 2 *A* and *B*). By FACS analysis, we also found that most of the p53-positive cells were in the G2/M stage of the cell cycle (Fig. 2*C*).

Second, healer and nonhealer tissues were examined. Histological sections from normal uninjured MRL and B6 ear tissue and small intestine were processed for immunohistochemistry (IHC). p53 expression is seen in normal MRL tissue (Figs. 2 *E*, *G*, *I*, and *K*) but is lower or not detectable in B6 tissue (Figs. 2 *D*, *F*, *H*, and *J*). This is supported by Western analysis of normal ear tissue (Fig. 2*L*).

To further explore the role of p53 during the regenerative process in vivo, ear hole closure assays were performed on B6 and MRL mice. Extracts from healing ear tissue on day 0, 5, and 10 postinjury were monitored for p53 expression using Western blotting (Fig. 2*M*). p53 protein levels were increased before and during healing in tissue from MRL compared to B6, showing that this increase in expression accompanies the healer phenotype. These data suggest that a cell cycle checkpoint response may be active at steady state and during healing.

Spontaneous DNA Damage Foci in MRL Healer Mice in Vitro and in Vivo. The DNA damage response cascade is enacted by two large kinases, ATM and ATR, which respond to various cellular stresses. An early hallmark of an active DNA damage response is the phosphorylation of the variant histone H2AX on the serine 139 residue or (γH2AX) (26). Using immunofluorescence, in vitro cultured MRL and congenic cells derived from normal uninjured ear tissue showed greater numbers of γH2AX foci than control B6 cells (Fig. 3*A*, white bars) including higher numbers of foci-positive cells and higher numbers of foci per cell. As a control, γ-irradiated (1 Gy, Fig. 3*A*, black bars) cells showed increased γH2AX foci after irradiation.

Tissue from uninjured ear and small intestine was also examined by IHC (Fig. 3*B*). MRL tissue displayed a greater level of γH2AX staining compared to B6 tissue. Protein extracts from cultured ear cells and chromatin-enriched ear tissue also demonstrated high levels of γH2AX levels by Western blot analysis (Fig. 3*C*), reaffirming an active DNA damage response in MRL and congenic normal uninjured cells, both in vitro and in vivo.

The histone protein H2AX can be phosphorylated proximal to DNA DSB after exposure to clastogenic agents, such as ionizing radiation, but also after replication-associated DSB that occur when gaps or single stranded regions are present in front of an advancing replication fork. The DNA damage response pathway that generally governs and protects against so-called replication stress is maintained by the ATR kinase. This kinase is activated by the TopBP1 protein (27). We analyzed the normal uninjured ear-derived cells for increased TopBP1 foci by IHC to further determine an association with an active replication stress response. Like γH2AX, TopBP1 foci were markedly enriched in the healer cells, indicative of an active and constitutive DNA damage checkpoint (Fig. 3*D*).

Cells from Healer Mice Display Elevated Levels of Endogenous DNA Damage. Numerous cellular stresses converge upon p53 activation and DNA damage response pathways. To test for bona fide DNA

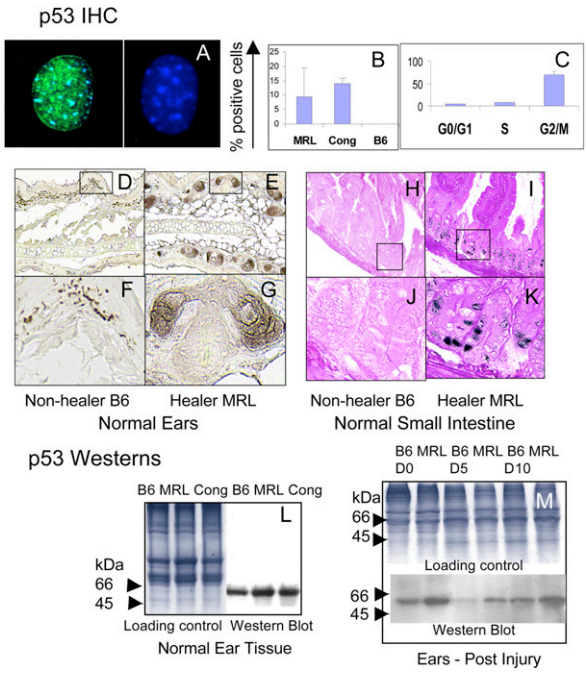

Fig. 2. p53 expression in cells and in both normal and injured tissue. Cells from healer mice (MRL, cong) and nonhealer mice (B6) were cultured on coverslips and then stained with DO1 anti-p53 antibody and anti-mouse Ig + DAPI. (*A*) p53 nuclear staining (anti-p53 is green and DAPI is blue) in an MRL cell (*Left*) and a B6 cell (*Right*). (*B*) The percent p53-positive cells in MRL, cong, and B6 cultured dermal cells. (*C*) The percentage of p53-positive cells at each stage of the cell cycle is indicated for the MRL cell line. Cells were stained with Vybrant Orange, separated by flow cytometry into three cell cycle stages, G0/G1, S, and G2/M. These cells were then put on slides and stained with antibody to p53. (*D–K*) shows histological sections of normal ear and small intestine from nonhealer (B6) (*D*, *F*, *H*, and *J*) and healer (MRL) mice (*E*, *G*, *I*, and *K*), which were stained with anti-p53 antibody + DAB. Western blots from normal B6, MRL, and congenic ear tissue along with Coomassie-stained gels as tissue loading controls are shown (*L*). Samples were run on a 14% SDS/PAGE gel and stained with anti-p53 antibody. Tissues from B6 and MRL injured ears (*M*) from *Left* to *Right* (B6, MRL day 0, 5, and 10). Above the p53 gel is a Coomassie blue-stained gel as a tissue loading control run per lane.

damage, we performed a comet assay at both neutral conditions (detecting DSB alone) and alkaline conditions [detecting both single strand breaks (SSB) and DSB]. The alkaline comet results showed high numbers of comets from MRL and other healer cells derived from normal uninjured ear tissue (an average of 80% comet positive) with large tail moments (Fig. 4*A* and Table S2). This is in contrast to few or no comets in nonhealer cells. These results agree with the γH2AX foci findings. The neutral comet assay (DSB only) counts were lower than the alkaline (DSB and SSB) counts but still averaged 35% comet-positive cells in the healers.

Increased Rad51 Foci in Healer Cells. Cells involved in regeneration of tissue should be proliferation-competent and the endogenous DNA damage observed must be repaired. There are two major pathways responsible for DNA DSB repair. Nonhomologous end joining can occur throughout the cell cycle but may be error prone. Homologous recombination, although, is error free and uses a sister chromatid as a template for repair during late S or G2 phases of the cell cycle. Because we observed a G2/M accumulation of MRL cells, we tested whether homologous recombination pathways were up-regulated to repair the endogenous damage. We found Rad51 foci increased in 10–15% of in vitro cultured healer cells compared to 1–2% nonhealer cells (Fig. 4*B*).

Healer Cells in Vivo Have Increased Markers of Apoptosis. Although many of the healer cells are repairing the intrinsic DNA damage, others clearly have a different outcome. To examine apoptosis, we examined caspase 3 and TUNEL. MRL tissue showed increased caspase 3 by Western blotting using extracts from small intestine and IHC staining of uninjured ear tissue (Fig. 4*C*). An increase in TUNEL-positive cells in MRL small intestine was also seen (Fig. 4*D*). Although the regeneration process requires cell proliferation, it appears to come at a cost to many cells in the population as markers of apoptosis were distinctly increased in healer cells.

Lack of p21 Expression/Induction in Healer Cells in Vitro. The pronounced intrinsic DNA damage in healer cells was strikingly consistent with recent reports showing that mouse embryonic stem cells display endogenous DNA damage and a faulty G1 checkpoint (23, 28). In those reports, a lack of checkpoint control was attributed in part to a lack of p21 induction. We therefore tested the hypothesis that the MRL healer cells also did not induce the p21 checkpoint protein. In comparison with both a human cell line (HCT116) and a mouse nonhealer cell line (B6), MRL cells did not display p21 protein expression and, furthermore, expression was not induced after DNA damage following ionizing radiation (Fig. 4*E*).

Deletion of p21 Converts a Nonhealer into a Regeneration-Competent Healer Mouse. Because p21 was down-regulated in healer cells, we asked whether the deletion of p21 would permit appendage regeneration potential in vivo in a nonregenerating mouse. We examined CDKN1A (p21)$^{-/-}$ mice (29) for ear hole closure over a one month period. The background control strain B6129SF2/J mice were ear punched in parallel and the data compared to MRL and B6 ear hole closure. As seen in Fig. 5*A*, ear hole closure in 6- to 7-wk-old p21$^{-/-}$ mice was almost identical to that seen in MRL healer mice, healing only slightly less well than MRLs on day 28. Age-matched p21$^{+/+}$ controls did not close and were similar to B6 nonhealer mice. Gross and histological analysis of the p21$^{-/-}$ ear holes over time showed closing holes with normal dermis, epidermis, and cartilage interspersed with thickened areas of dermis (Fig. 5 *B–H*). To further establish the link between G1 checkpoint control and the regeneration phenotype, cells derived from the ear pinnae of normal uninjured p21$^{+/+}$ and p21$^{-/-}$ mice were examined for DNA damage and cell cycle arrest. γH2AX staining (Fig. 5 *I*, *J*, and *M*), comet formation (Fig. 5 *K*, *L*, *M*), and increased levels of cells in G2/M (Fig. 5*N*) were found in the p21$^{-/-}$ mice compared to the p21$^{+/+}$ mice. This directly correlated with what was seen in the healer MRL, congenic, and RI mouse cells described above in vivo and in vitro, solidifying the role of p21 underexpression and tissue and appendage regeneration.

Discussion

Many mammals, including humans and most mouse strains, are capable of tissue regeneration to varying degrees. This ranges from the replacement of extensively resected liver lobes to the interstitial replacement of damaged skeletal muscle cells, epithelium, the gut lining, and a modest life-long replacement of CNS neurons and cardiomyocytes. In contrast, with few exceptions (ear hole closure in rabbits and seasonal antler replacement), the regeneration of lost appendage tissue is virtually never seen. The key observation of this paper is that the MRL mouse strain (and close relatives), unique among mice in their ability to close ear holes, shows high levels of DNA damage, a G2/M bias, and a lack of p21 protein expression in both uninjured steady state tissue and postinjury. The functional role of p21 has been demonstrated in a p21 knockout mouse, which displays the same range of cellular effects as seen in the MRL mouse and reproduces appendage regeneration in vivo.

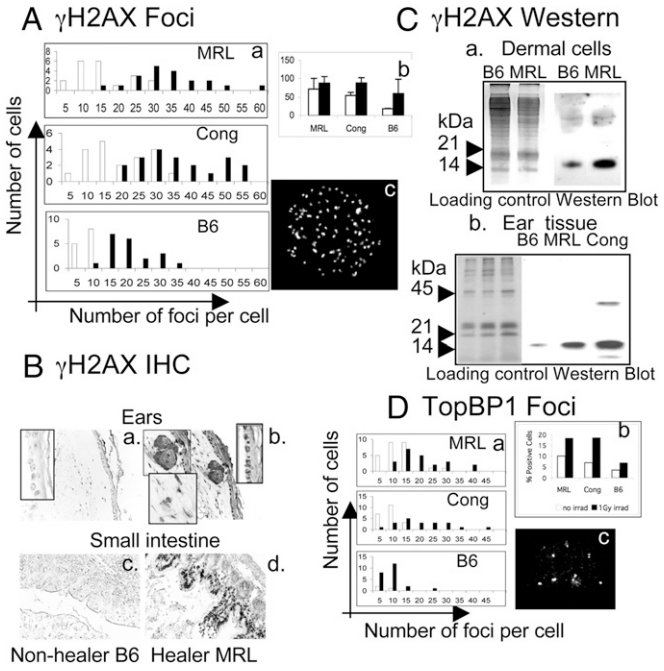

Fig. 3. Detection of γH2AX and TopBP1 foci in cells and normal tissue. Dermal cells from healer mice (MRL, Cong) and nonhealer mice (B6) were cultured on coverslips and then stained with antiphospho-histone H2AX). White bars are normal cells, black bars are irradiated cells (1 Gy). (*A*) The number of foci/cell by counting 20 nuclei/cell line at 60× is presented as three histograms (*Aa*) with MRL (*Top*); Congenic (*Middle*), and B6 (*Bottom*). (*Ab*) Percentage of γH2AX-positive cells determined by counting between 100–200 cells/treatment. (*Ac*) A representative γH2AX-stained MRL cultured dermal cell nucleus with foci. (*Ba–d*) Tissue sections from ear and small intestine of normal B6 and MRL mice treated with γH2AX antibody and DAB stains hair follicles, dermal and basal epidermal cells in the ear, and villous epidermal cells in the small intestine. (*Ca*) Western analysis of ear-derived dermal cells and (*Cb*) ear tissue is shown using chromatin-enriched tissue run on a 14% SDS/PAGE gel. (*Ca*) Loading controls for cells (lanes 1, 2) stained with Coomassie blue; γH2AX bands (lanes 3, 4) seen at approximately 15 kDa. (*Cb*) Loading controls for tissue stained with Coomassie blue (lanes 1–3); γH2AX bands (lanes 4–6). (*D a* and *b*) A similar analysis of TopBP1 staining of nuclear foci. (*Dc*) TopBP1 foci are seen in an MRL dermal cell nucleus.

Association of Healing, G2/M Arrest, and DNA Damage. These studies explore the autoimmune-prone MRL mouse (25), which has unusual healing and regenerative responses after wounding. We have shown here that dermal cells derived from ear pinnae of normal uninjured but regeneration-competent mice show a cell cycle response in culture in which elevated numbers of cells are found in G2/M. This is accompanied by various markers of DNA damage and repair responses including the direct detection of single and double strand DNA breaks (comet assay), an increase in phosphorylated H2AX, TopBP1, Rad51 foci formation, and elevated p53. The comet assay results confirm DNA damage response molecular markers and also show a massive accumulation of DNA SSB and DSB in healer cells. This is in contrast to the cell cycle response of cells from nonregenerating mice including cells from B6, SM/J, and (LG/J × SM/J) recombinant inbred nonhealing mice, which show the majority of cells in G0/G1 and without a constitutively active DNA damage/repair response and DNA damage.

G2/M Arrest in Regenerating Models. The preponderance of healer cells in G2/M has several parallels in other animals and mammalian tissues capable of regeneration. Hydra, a classic regenerator, has been shown to have a large number of cells in G2/M, especially those in the most regenerative part of the organism (15–18), and estimated to be about 68% of all cells (15). Because terminal differentiation of cells in the hydra can occur from G2, this arrested state is functional (16). A similar result has been reported in planaria (30) and in adult urodele amphibians (e.g., the newt) that can regenerate limbs. In vitro experiments using newt cells show cell cycle reentry, local dedifferentiation, and proliferation (2, 19). Newts have also been shown to have many cells in G2 (31). Most recently, a proteomics study in regenerating axolotl limbs also suggests potential G2 arrest (32). Thus, G2/M arrest appears to be a common finding in regenerating organisms.

In the regenerating mammalian liver, polyploidy is a dominant feature in adult hepatocytes, where up to 70% are tetraploid (33). These cells can be binuclear or mononuclear (34). Also, G2/M arrest is seen in stem cells (21). Why there is a predominance of cells in G2 in tissue capable of a regenerative response is unclear. However, there is evidence that senescent cells [i.e., cells that display similar characteristics of G2/M arrest and a DNA damage response in vitro and in vivo (35, 36)] make proinflammatory cytokines and proteases that may lead to a microenvironment that is positive for cell growth (37, 38). Cells in G2/M could provide a milieu that would enhance a proliferative response once initiated, a response important in self-renewal and regeneration.

DNA Damage Responses, Hyperproliferation, and Apoptosis. Why is there activation of a DNA damage response in normal tissues of the MRL mouse and related healing strains? MRL mice have been reported to have a mutation in *exoI*, which is involved in mismatch repair of DNA replication (39). Hence, the exoI mutation may contribute to an accumulation of DNA damage and to G2/M arrest, but it remains unclear how this promotes organ regeneration. Some insight is suggested by a mouse model in which the catalytic subunit of telomerase is deleted. This mouse displays organ failure and defects in maintenance of cell proliferation but can be rescued by an exoI deficiency leading to prolonged lifespan, suggesting a role for exoI mutations in the cellular regeneration phenotype (40).

It is generally thought that certain areas of the genome are especially prone to difficulties in DNA replication and that this stress can trigger the activation of the DNA damage response. It has been reported that constitutive DNA damage and DNA damage responses occur in hyperplastic cells in precancerous tissues (41). Thus, our data suggest that highly regenerative cells resemble the hyperproliferative cells seen in early stages of carcinogenesis. We also observed an increase in cellular apoptosis in regenerative cells. The combined effects of increased proliferation and apoptosis may allow the organism to eliminate old cells and keep the cell turnover rate high as seen, for example, during development in the brain and thymus. Similar increases in apoptosis occur in planaria, *Xenopus*, and in newt during regenerative responses (42–44).

The intrinsic DNA damage and subsequent G2/M arrest displayed here also activates the homologous recombination pathway, biasing DNA repair pathways toward an error-free mechanism of repair that may be important in maintaining genome stability of newly formed tissues and cells. In support of this idea is the fact that elevated levels of homologous recombination are also seen in the regeneration of rat liver tissue (45).

The lack of p21 expression displayed in our system may be analogous to a diminished checkpoint response necessary for enhanced induced pluripotential stem (iPS) cell formation. A recent report showed that a p53/p21 DNA damage response leading to G1 arrest suppresses iPS formation and that a distinct gene expression profile is required for a stem cell state (46). Tissue regeneration in mice is likely mediated by a stem cell-like phenotype. The same may be true for the MRL mouse, as a distinct G2/M genetic program may need to be initiated for tissue regeneration. In fact, cells positive for Nanog and Sox2 are increased in MRL mouse tissue (47). Although some level of

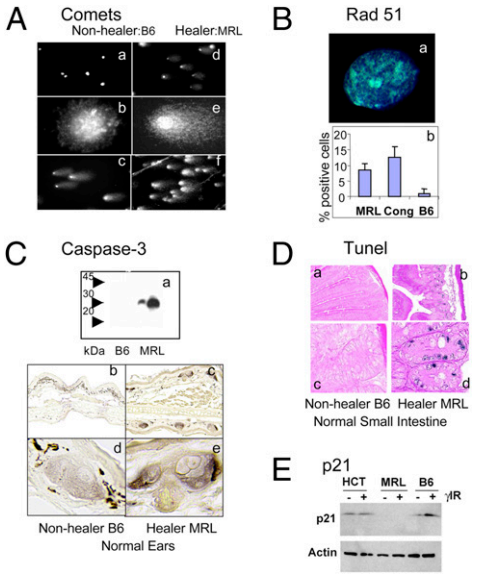

Fig. 4. Functional analysis of DNA damage and repair. (*Aa–f*) Ear dermal cells from nonhealer B6 and healer MRL mice were tested for DNA damage using the comet assay under alkaline conditions. Comets can be seen in MRL cells at 10× (*Ad*) and 60× (*Ae*) magnification but not in B6 cells (*A a* and *b*, respectively). (*A c* and *f*) After 10 Gy γ-irradiation, all B6 and MRL cells display comet formation. (*B*) Analysis of Rad 51. (*Ba*) Rad51 foci in an MRL healer cell; (*Bb*) percent Rad51-positive cells in MRL, Cong, and B6 cells. (*Ca*) Western analysis of caspase protein on a 12% SDS/PAGE gel of B6 and MRL tissue samples from small intestine (two samples each) with expression only in MRL. (*C b–d*) Histological sections from nonhealer (B6) and healer (MRL) ears stained with antibody to the active form of caspase 3. (*D a–d*). Sections from small intestine were examined by TUNEL at 10× (*D a* and *b*) and 60× magnification (*D c* and *d*). (*E*) Western analysis of p21 expression in a human cell line (HCT116), in MRL healer cells, and B6 nonhealer cells in the absence and presence of ionizing irradiation (1 Gy).

DNA damage can be tolerated during cellular reprogramming, apoptosis can ensue if the levels are too high (48). In the MRL system, persistent DNA damage does occur, leading to apoptosis in a subset of the MRL cell population.

Central Role for p21. All of the effects observed in this study can be explained by the lack of p21 induction in healer cells. This observation may have numerous consequences that lead to the regeneration phenotype. First, without the p21 protein, a G1 checkpoint cannot be fully enacted, leading to a dependency on the G2 checkpoint and explains the remarkable cell cycle profiles of healer cells. Second, without p21, unscheduled entry into S-phase occurs and enhanced proliferation is seen. In fact, in a recent study examining p21 deletion in human fibroblasts, up-regulation of p53 with enhanced proliferation and replication stress is observed similar to the results seen in our regeneration phenotype (49). Third, increased DNA damage is reported in cells lacking p21 and is probably due to proliferative and replicative stress (49). The inability to enter quiescence at G0 in response to stress leads to G2 arrest, which is also observed in MRL mice.

Other studies have also provided evidence that cell cycle control is important for the regeneration phenotype. In vitro regenerative potential is associated with hyperphosphorylation of Rb in newt myotube cultures (19) and in $Rb^{-/-}$ mouse myotubes (50). These two cases would be functionally similar to the absence of p21, where cyclin-cdk interactions would not be inhibited and would thus bypass the G1 checkpoint. In vivo, the absence of p21 has been shown in double mutant mice to both enhance liver regeneration and muscle cell proliferation (51–53). However, in both cases, these tissues normally regenerate.

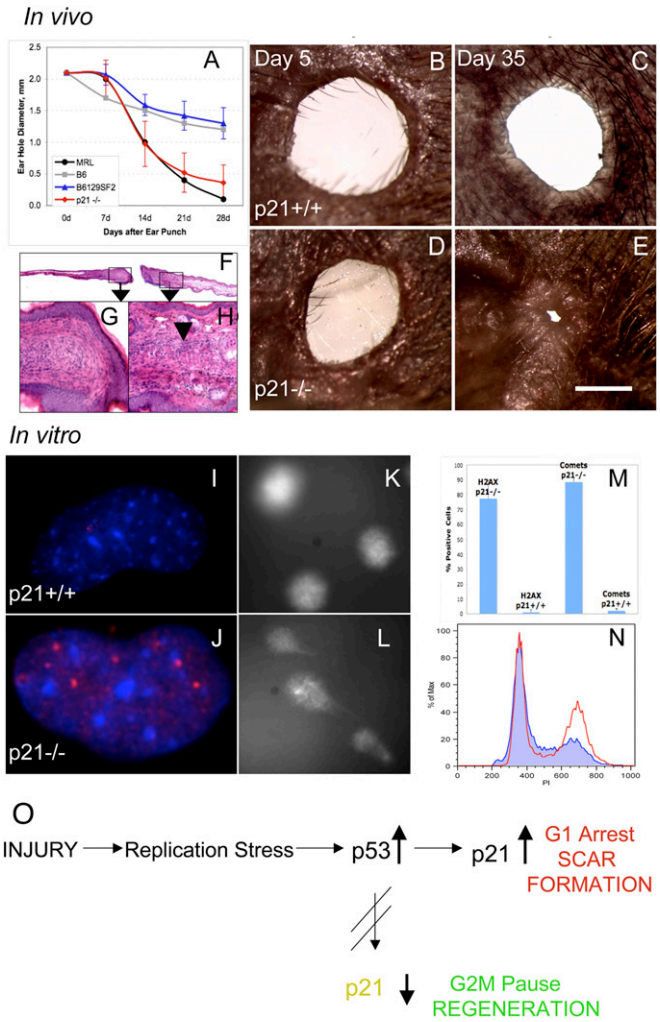

Fig. 5. P21 knockout mouse ear hole closure. (*A*) Ear pinnae of p21 KO ($CDKN1A^{-/-}$) and WT (B6129F2) control female mice were ear punched and the mean hole diameters ± SD measured. Ear hole closure of KO ($n = 10 \times$ two ears) and WT mice ($n = 9 \times$ two ears) is compared to B6 and MRL hole diameters and shown weekly over a 1 month period. (*B* and *C*) Photographs of $p21^{+/+}$ ear holes (day 5 and 35 postinjury, respectively) and (*D* and *E*) photographs of $p21^{-/-}$ ear holes (day 5 and 35 postinjury, respectively) can be seen. (Scale bar: 1mm.) (*F–H*) Histological analysis shows $p21^{-/-}$ ear hole tissue on day 35. (*F*) Ear tissue extending from the cut cartilage (4×). (*G*) Normal blastema-like tissue (40×) and (*H*) condensations extending from the cut cartilage can be seen (arrow: 40×). (*I–N*) Analysis of cells from the ear pinnae of $p21^{+/+}$ mice and $p21^{-/-}$ mice for (*I* and *J*) γH2AX staining (DAPI = blue; anti-γH2AX = red), (*K* and *L*) comets. (*M*) Cells were counted for both γH2AX staining and comets and percent positive cells + SD determined. (*N*) Cell cycle analysis (using propidium iodide) was carried out with the $p21^{-/-}$ cells in red and $p21^{+/+}$ cells in blue. (*O*) Model describing the links between cell cycle checkpoint control, proliferation, and the tissue regeneration phenotype. After tissue injury such as an ear hole punch, hyperproliferation ensues. In WT or p21-proficient cells, a G1 checkpoint is enacted leading to scar formation. In p21-defective cells such as those derived from the MRL strain and $p21^{-/-}$ mice, rounds of unscheduled DNA synthesis can occur, leading to DNA damage and an abundance of DNA damage markers. A G2 checkpoint can be enacted, leading to enhanced tissue regeneration.

In our studies, p21 down-regulation plays a most striking role as deletion of this molecule alone establishes appendage regenerative competence in whole animals. Thus, using the ear hole closure model, the control WT mouse strain B6129SF2/J does not close ear holes, similar to other nonregenerating mice, although the CDKN1A $(p21)^{-/-}$ mouse strain does close ear holes and

displays morphological and histological regenerative responses similar to MRL mice. Interestingly, this same deletion shows another shared characteristic with the MRL mouse, that of a mild to severe manifestation of a lupus-like syndrome (54, 55). This correlation between regenerative potential and autoimmune state could suggest that in clinical autoimmune disease, a corresponding enhanced regenerative potential might be seen in some patients.

Methods

Animals. Commercially available mice were obtained from Jackson or Taconic Laboratories. Through-and-through ear hole punches were carried out as previously described (3). Please see *SI Text* for complete details.

Cell Culture, Cell Cycle Analysis, and Comet Assays. Primary skin dermal cells from ear pinnae were established and cells from early passages were used. These cells were analyzed for cell cycle using either Propidium Iodide (PI) dye (P-4170; Sigma) or Vybrant DyeCycle Orange (V35005; Molecular Probes) by flow cytometry. Comets were prepared using these cells as previously described (56).

IHC. Primary ear skin dermal cells were grown on glass coverslips and tissue from normal ears and from the small intestine were fixed and embedded. Staining with antibody is as described previously (6).

Western Blot Analysis. Western blot analysis was carried out for four different antigens (p53, γH2AX, caspase 3, p21, and actin as a control) using three different tissues (cultured dermal cells, ear pinnae, and small intestine).

TUNEL Analysis. Paraffin-embedded small intestine was analyzed using the DermaTACS In Situ Apoptosis Detection Kit (4829-30-K; Trevigen, Inc.).

ACKNOWLEDGMENTS. We would like to thank T. Halazonetis, R. Naviaux, T. Stomato, and L. Matthew Arthur for their thoughts and useful discussions. This work was supported by grants from the Harold G. and Leila Y. Mathers Foundation, the F.M. Kirby Foundation, the W.W. Smith Foundation, and National Institutes of Health Grants from National Institute of General Medical Sciences (GM073226) and the National Cancer Institute Cancer Center Grant (P30 CA10815). A.S. was supported by a grant from National Cancer Institute, National Institutes of Health.

1. Stocum DL (2004) Amphibian regeneration and stem cells. *Curr Top Microbiol Immunol* 280:1–70.
2. Brockes JP, Kumar A (2005) Appendage regeneration in adult vertebrates and implications for regenerative medicine. *Science* 310:1919–1923.
3. Clark LD, Clark RK, Heber-Katz E (1998) A new murine model for mammalian wound repair and regeneration. *Clin Immunol Immunopathol* 88:35–45.
4. Fitzgerald J, et al. (2008) Evidence for articular cartilage regeneration in MRL/MpJ mice. *Osteoarthritis Cartilage* 16:1319–1326.
5. Chadwick RB, et al. (2007) Digit tip regrowth and differential gene expression in MRL/Mpj, DBA/2, and C57BL/6 mice. *Wound Repair Regen* 15:275–284.
6. Gourevitch DL, Clark L, Bedelbaeva K, Leferovich J, Heber-Katz E (2009) Dynamic changes after murine digit amputation: The MRL mouse digit shows waves of tissue remodeling, growth, and apoptosis. *Wound Repair Regen* 17:447–455.
7. McBrearty BA, Clark LD, Zhang X-M, Blankenhorn EP, Heber-Katz E (1998) Genetic analysis of a mammalian wound-healing trait. *Proc Natl Acad Sci USA* 95:11792–11797.
8. Blankenhorn EP, et al. (2003) Sexually dimorphic genes regulate healing and regeneration in MRL mice. *Mamm Genome* 14:250–260.
9. Masinde GL, et al. (2001) Identification of wound healing/regeneration quantitative trait loci (QTL) at multiple time points that explain seventy percent of variance in (MRL/MpJ and SJL/J) mice F2 population. *Genome Res* 11:2027–2033.
10. Yu H, Mohan S, Masinde GL, Baylink DJ (2005) Mapping the dominant wound healing and soft tissue regeneration QTL in MRL x CAST. *Mamm Genome* 16:918–924.
11. Blankenhorn EP, et al. (2009) Genetic loci that regulate healing and regeneration in LG/J and SM/J mice. *Mamm Genome* 20:720–733.
12. Wiens M, Perović-Ottstadt S, Müller IM, Müller WE (2004) Allograft rejection in the mixed cell reaction system of the demosponge Suberites domuncula is controlled by differential expression of apoptotic genes. *Immunogenetics* 56:597–610.
13. Müller WE, et al. (2006) Novel mechanism for the radiation-induced bystander effect: Nitric oxide and ethylene determine the response in sponge cells. *Mutat Res* 597:62–72.
14. Martínez DE (1998) Mortality patterns suggest lack of senescence in hydra. *Exp Gerontol* 33:217–225.
15. Schmidt T, David CN (1986) Gland cells in Hydra: Cell cycle kinetics and development. *J Cell Sci* 85:197–215.
16. Dübel S, Schaller HC (1990) Terminal differentiation of ectodermal epithelial stem cells of Hydra can occur in G2 without requiring mitosis or S phase. *J Cell Biol* 110:939–945.
17. Holstein TW, Hobmayer E, David CN (1991) Pattern of epithelial cell cycling in hydra. *Dev Biol* 148:602–611.
18. Ulrich H, Tárnok A (2005) Quantification of cell-cycle distribution and mitotic index in Hydra by flow cytometry. *Cell Prolif* 38:63–75.
19. Tanaka EM, Gann AA, Gates PB, Brockes JP, Brockes JP (1997) Newt myotubes reenter the cell cycle by phosphorylation of the retinoblastoma protein. *J Cell Biol* 136:155–165.
20. Michalopoulos GK, DeFrances MC (1997) Liver regeneration. *Science* 276:60–66.
21. Chuykin IA, Lianguzova MS, Pospelova TV, Pospelov VA (2008) Activation of DNA damage response signaling in mouse embryonic stem cells. *Cell Cycle* 7:2922–2928.
22. Hong Y, Cervantes RB, Tichy E, Tischfield JA, Stambrook PJ (2007) Protecting genomic integrity in somatic cells and embryonic stem cells. *Mutat Res* 614:48–55.
23. Galvin KE, Ye H, Erstad DJ, Feddersen R, Wetmore C (2008) Gli1 induces G2/M arrest and apoptosis in hippocampal but not tumor-derived neural stem cells. *Stem Cells* 26:1027–1036.
24. Hrbek T, de Brito RA, Wang B, Pletscher LS, Cheverud JM (2006) Genetic characterization of a new set of recombinant inbred lines (LGXSM) formed from the inter-cross of SM/J and LG/J inbred mouse strains. *Mamm Genome* 17:417–429.
25. Murphy ED, Roths JB (1979) Autoimmunity and Lymphoproliferation: Induction by Mutant Gene lpr and Acceleration by a Male-Associated Factor in Strain BXSB. *Genetic Control of Autoimmune Disease*, eds Rose NR, Bigazzi PE, and Warner NL (Elsevier, New York), pp 207–220.
26. Rogakou EP, Pilch DR, Orr AH, Ivanova VS, Bonner WM (1998) DNA double-stranded breaks induce histone H2AX phosphorylation on serine 139. *J Biol Chem* 273:5858–5868.
27. Kumagai A, Lee J, Yoo HY, Dunphy WG (2006) TopBP1 activates the ATR-ATRIP complex. *Cell* 124:943–955.
28. Hong Y, Stambrook PJ (2004) Restoration of an absent G1 arrest and protection from apoptosis in embryonic stem cells after ionizing radiation. *Proc Natl Acad Sci USA* 101:14443–14448.
29. Brugarolas J, et al. (1995) Radiation-induced cell cycle arrest compromised by p21 deficiency. *Nature* 377:552–557.
30. Saló E, Baguñà J (1984) Regeneration and pattern formation in planarians. I. The pattern of mitosis in anterior and posterior regeneration in Dugesia (G) tigrina, and a new proposal for blastema formation. *J Embryol Exp Morphol* 83:63–80.
31. Tassava RA, Mescher AL (1976) Mitotic activity and nucleic acid precursor incorporation in denervated and innervated limb stumps of axolotl larvae. *J Exp Zool* 195:253–262.
32. Rao N, et al. (2009) Proteomic analysis of blastema formation in regenerating axolotl limbs. *BMC Biol* 7:83–108.
33. Van Bezooijen CF, Van Noord MJ, Knook DL (1974) The viability of parenchymal liver cells isolated from young and old rats. *Mech Ageing Dev* 3:107–119.
34. Guidotti JE, et al. (2003) Liver cell polyploidization: A pivotal role for binuclear hepatocytes. *J Biol Chem* 278:19095–19101.
35. von Zglinicki T, Saretzki G, Ladhoff J, d'Adda di Fagagna F, Jackson SP (2005) Human cell senescence as a DNA damage response. *Mech Ageing Dev* 126:111–117.
36. Herbig U, Ferreira M, Condel L, Carey D, Sedivy JM (2006) Cellular senescence in aging primates. *Science* 311:1257.
37. Campisi J (1998) The role of cellular senescence in skin aging. *J Investig Dermatol Symp Proc* 3:1–5.
38. Parrinello S, Coppe JP, Krtolica A, Campisi J (2005) Stromal-epithelial interactions in aging and cancer: Senescent fibroblasts alter epithelial cell differentiation. *J Cell Sci* 118:485–496.
39. Namiki Y, Endoh D, Kon Y (2003) Genetic mutation associated with meiotic metaphase-specific apoptosis in MRL/MpJ mice. *Mol Reprod Dev* 64:179–188.
40. Schaetzlein S, et al. (2007) Exonuclease-1 deletion impairs DNA damage signaling and prolongs lifespan of telomere-dysfunctional mice. *Cell* 130:863–877.
41. Gorgoulis VG, et al. (2005) Activation of the DNA damage checkpoint and genomic instability in human precancerous lesions. *Nature* 434:907–913.
42. Hwang JS, Kobayashi C, Agata K, Ikeo K, Gojobori T (2004) Detection of apoptosis during planarian regeneration by the expression of apoptosis-related genes and TUNEL assay. *Gene* 333:15–25.
43. Mescher AL, White GW, Brokaw JJ (2000) Apoptosis in regenerating and denervated, nonregenerating urodele forelimbs. *Wound Repair Regen* 8:110–116.
44. Tseng AS, Adams DS, Qiu D, Koustubhan P, Levin M (2007) Apoptosis is required during early stages of tail regeneration in Xenopus laevis. *Dev Biol* 301:62–69.
45. Thyagarajan B, Cruise JL, Campbell C (1996) Elevated levels of homologous DNA recombination activity in the regenerating rat liver. *Somat Cell Mol Genet* 22:31–39.
46. Hong H, et al. (2009) Suppression of induced pluripotent stem cell generation by the p53-p21 pathway. *Nature* 460:1132–1135.
47. Naviaux RK, et al. (2009) Retained features of embryonic metabolism in the adult MRL mouse. *Mol Genet Metab* 96:133–144.
48. Marión RM, et al. (2009) A p53-mediated DNA damage response limits reprogramming to ensure iPS cell genomic integrity. *Nature* 460:1149–1153.
49. Perucca P, et al. (2009) Loss of p21 CDKN1A impairs entry to quiescence and activates a DNA damage response in normal fibroblasts induced to quiescence. *Cell Cycle* 8:105–114.
50. Schneider JW, Gu W, Zhu L, Mahdavi V, Nadal-Ginard B (1994) Reversal of terminal differentiation mediated by p107 in Rb-/- muscle cells. *Science* 264:1467–1471.
51. Stepniak E, et al. (2006) c-Jun/AP-1 controls liver regeneration by repressing p53/p21 and p38 MAPK activity. *Genes Dev* 20:2306–2314.
52. Willenbring H, et al. (2008) Loss of p21 permits carcinogenesis from chronically damaged liver and kidney epithelial cells despite unchecked apoptosis. *Cancer Cell* 14:59–67.
53. Hawke TJ, Jiang N, Garry DJ (2003) Absence of p21CIP rescues myogenic progenitor cell proliferative and regenerative capacity in Foxk1 null mice. *J Biol Chem* 278:4015–4020.
54. Balomenos D, et al. (2000) The cell cycle inhibitor p21 controls T-cell proliferation and sex-linked lupus development. *Nat Med* 6:171–176.
55. Santiago-Raber ML, et al. (2001) Role of cyclin kinase inhibitor p21 in systemic autoimmunity. *J Immunol* 167:4067–4074.
56. Speit G, Hartmann A (2006) The comet assay: A sensitive genotoxicity test for the detection of DNA damage and repair. *Methods Mol Biol* 314:275–286.